

The Dof Transcription Factor OBP3 Modulates Phytochrome and Cryptochrome Signaling in *Arabidopsis*^W

Jason M. Ward, Carie A. Cufr, Megan A. Denzel, and Michael M. Neff¹

Department of Biology, Washington University, St. Louis, Missouri 63130

Plants perceive subtle changes in light quality and quantity through a set of photoreceptors, including phytochromes and cryptochromes. Upon perception, these photoreceptors initiate signal transduction pathways leading to photomorphogenic changes in development. Using activation-tagging mutagenesis to identify novel light-signaling components, we have isolated a gain-of-function mutant, *sob1-D* (suppressor of *phytochrome B-4* [*phyB-4*] dominant), which suppresses the long-hypocotyl phenotype of the *phyB* missense allele, *phyB-4*. The *sob1-D* mutant phenotype is caused by the overexpression of a Dof (DNA binding with one finger) transcription factor, *OBP4 Binding Protein 3* (OBP3). A translational fusion between OBP3 and green fluorescent protein is nuclear localized in onion (*Allium cepa*) cells. Tissue-specific accumulation of an OBP3:OBP3-β-glucuronidase translational fusion is regulated by light in *Arabidopsis thaliana*. Hypocotyls of transgenic lines with reduced OBP3 expression are less responsive to red light. This aberrant phenotype in red light requires functional *phyB*, suggesting that OBP3 is a positive regulator of *phyB*-mediated inhibition of hypocotyl elongation. Furthermore, these partial-loss-of-function lines have larger cotyledons. This light-dependent cotyledon phenotype is most dramatic in blue light and requires functional cryptochrome 1 (*cry1*), indicating that OBP3 is a negative regulator of *cry1*-mediated cotyledon expansion. These results suggest a model where OBP3 is a component in both *phyB* and *cry1* signaling pathways, acting as a positive and negative regulator, respectively. An alternate, though not mutually exclusive, model places OBP3 as a general inhibitor of tissue expansion with *phyB* and *cry1*, differentially modulating OBP3's role in this response.

INTRODUCTION

Plants must respond to several environmental cues, one of the most important being light. Not only required for photosynthesis, light is used by plants to determine their location in relation to each other. Changes in light quality or quantity are perceived by a set of photoreceptors characterized by the wavelength they absorb. These include the red/far-red absorbing phytochromes, the blue/UV-A absorbing cryptochromes and phototropins, and the as of yet unidentified UV-B photoreceptors (Nagy and Schafer, 2002; Lin and Shalitin, 2003).

In *Arabidopsis thaliana*, there are five phytochromes (*phy*), at least three cryptochromes (*cry*), and two phototropins. The phototropins mediate responses such as phototropism, chloroplast movement, and changes in stomatal aperture (Briggs and Christie, 2002). The phytochromes and cryptochromes have both unique and redundant roles in mediating photomorphogenic responses, including hypocotyl elongation, cotyledon/leaf expansion, flowering time, and regulation of gene expression (Neff et al., 2000; Lin and Shalitin, 2003).

Photomorphogenic signaling in far-red and red light is mediated mainly by phytochrome A (*phyA*) and *phyB*, respectively. However, other phytochromes mediate the red light response as

well (Franklin et al., 2003; Monte et al., 2003). All phytochromes are synthesized, in their inactive form, in the cytoplasm and undergo red light-dependent photoconversion to their active form. A portion of the active phytochromes remain in the cytoplasm where signaling can occur through interactions with proteins such as Phytochrome Kinase Substrate 1 (Fankhauser et al., 1999). Active phytochromes can also undergo translocation into the nucleus to initiate further signal transduction. *phyB* is thought to initiate signal transduction through its C terminus, which is responsible for interactions with other proteins, including photoreceptors and transcription factors (Ni et al., 1998; Mas et al., 2000). However, the *phyB* C terminus may not be required for all *phyB*-mediated signaling (Matsushita et al., 2003). Many transcription factors are involved in *phyB*-mediated signal transduction, including Phytochrome Interacting Factor 3 (PIF3), Long Hypocotyl 5, Dof Affecting Germination 1 (DAG1), DAG2, and Cogwheel 1 (COG1) (Ni et al., 1998; Osterlund et al., 2000; Gualberti et al., 2002; Park et al., 2003).

In blue light, photomorphogenic responses are mediated primarily by cryptochrome 1 (*cry1*) and *cry2*. *cry1* is responsible for seedling deetiolation in high fluence rates of light, and *cry2* mediates flowering time and deetiolation in response to lower fluence rates (Koomneef et al., 1980; Ahmad and Cashmore, 1993; Lin et al., 1998). The C terminus of the cryptochromes contains domains responsible for subcellular localization, protein-protein interactions, and physiological function. There is evidence that phytochromes and cryptochromes work together, either through interactions with each other (Mas et al., 2000; Jarillo et al., 2001) or via common signaling components, such as Long Hypocotyl in Far-Red 1 (HFR1) and Short Under Blue Light 1 (SUB1) (Guo et al., 2001; Duek and Fankhauser, 2003).

¹To whom correspondence should be addressed. E-mail: mneff@biology2.wustl.edu; fax 314-935-4432.

The author responsible for distribution of materials integral to the findings presented in this article in accordance with the policy described in the Instructions for Authors (www.plantcell.org) is: Michael M. Neff (mneff@biology2.wustl.edu).

^WOnline version contains Web-only data.

Article, publication date, and citation information can be found at www.plantcell.org/cgi/doi/10.1105/tpc.104.027722.

Several signaling components downstream of the phytochromes and cryptochromes have been identified using a variety of approaches. We have used activation-tagging mutagenesis to identify novel components involved in light signaling. Using this approach, we have identified a new mutation, *sob1-D* (suppressor of *phyB-4* dominant), which suppresses the long-hypocotyl phenotype of *phyB-4*. The *sob1-D* mutant phenotype is caused by the overexpression of a Dof (DNA binding with one finger) transcription factor, previously named *OBF4 Binding Protein 3* (*OBP3*) (Kang and Singh, 2000).

OBP3 binds DNA in a sequence-specific manner and is able to activate transcription in a transient assay (Kang and Singh, 2000). *OBP3* expression levels are regulated by salicylic acid and auxin (Kang and Singh, 2000). Hypermorphic alleles, overexpressing *OBP3*, are severe dwarfs, suggesting an involvement in plant development (Kang and Singh, 2000). However, this hypothesis has not been tested with hypomorphic alleles. Through characterization of transgenic lines with reduced *OBP3* expression, we have uncovered a role for this gene in *phyB*-mediated inhibition of hypocotyl elongation in red light and *cry1*-mediated cotyledon expansion in blue light.

RESULTS

The *sob1-D* Mutant, Caused by the Overexpression of *OBP3*, Suppresses the Long-Hypocotyl Phenotype of *phyB-4*

The *Arabidopsis* *phyB-4* mutation, caused by a single amino acid change near the chromophore binding site, confers a long-hypocotyl phenotype when compared with the wild type (Koornneef et al., 1980; Reed et al., 1993; Elich and Chory, 1997). In an activation-tagging mutagenesis of ~7000 primary transformants (T1), we identified and cloned the genes causing four independent, gain-of-function mutations that suppress the long-hypocotyl phenotype of *phyB-4*. This study focuses on one of these mutants identified in our lab, *sob1-D*.

The *sob1-D phyB-4* double mutant had a dramatically shorter hypocotyl than the *phyB-4* mutant and the wild type when grown in white light (Figure 1A). However, the double mutant elongated normally in the dark, suggesting that the gene altered in this mutant is involved in light signaling (Figure 1A). Both the *sob1-D phyB-4* double mutant and *sob1-D* single mutant were severe dwarfs with reduced fertility as adults (Figure 1B; data not shown). DNA gel blot and segregation analysis indicated that there was one T-DNA in the *sob1-D phyB-4* mutant, and it was genetically linked to the mutant phenotype.

Genomic DNA flanking the T-DNA insertion was cloned via plasmid rescue. Sequencing and subsequent BLAST analysis (Altschul et al., 1990) of a portion of the cloned DNA indicated that the T-DNA was inserted into chromosome III. The closest open reading frame is ~1 kb 5' from the left border of the T-DNA. Sequencing and PCR analysis confirmed that all four copies of the enhancers were inserted 1139 bp 3' of the stop codon of a Dof transcription factor previously named *OBP3* (Figure 1C; Kang and Singh, 2000).

RT-PCR demonstrated that *OBP3* is overexpressed in the *sob1-D phyB-4* mutant (Figure 1D). To confirm that *OBP3* overexpression causes the *sob1-D* mutant phenotype, the *phyB-4*

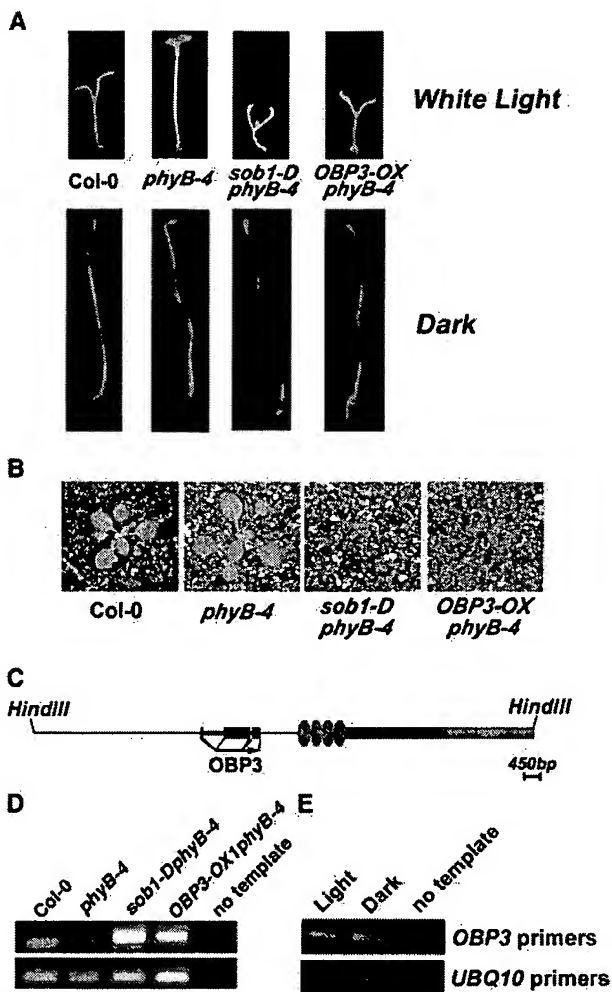


Figure 1. Phenotypic Analysis of the *sob1-D* Mutant and Cloning of the *SOB1* Gene.

(A) Seedlings were grown in continuous white light (35 μ M/m²/s) or in the dark for 5 d.

(B) Three-week-old plants were grown in long-day (16 h light/8 h dark) growth conditions.

(C) A diagram of the DNA that was cloned by plasmid rescue. The diagram shows the insertion site relative to the *OBP3* coding region and the restriction sites used to clone the DNA. The red ovals represent the four enhancers from the CaMV 35S promoter present in the T-DNA, the blue and green bars represent pBluescript KS+ and *nptII*, respectively.

(D) Total RNA was isolated from 5-d-old seedlings grown in continuous white light. PCR was performed on cDNA using *OBP3*-specific primers for 32 cycles. The *UBQ10* cDNA, amplified for 24 cycles, was used to normalize the amount of cDNA in each of the samples.

(E) RT-PCR was performed on total RNA isolated from 5-d-old seedlings grown in continuous white light or in the dark. PCR was performed as described in (D).

mutant was transformed with genomic DNA encoding *OBP3* along with the four enhancers. Transgenic lines with increased *OBP3* expression recapitulated the original *sob1-D* mutant phenotypes (Figures 1A, 1B, and 1D), indicating that the over-expression of *OBP3* is responsible for suppressing the long-hypocotyl phenotype of *phyB-4* in the *sob1-D phyB-4* double mutant.

OBP3 Is Nuclear Localized

Based on sequence similarity, *OBP3* is a putative Dof transcription factor (Kang and Singh, 2000). In addition, an *OBP3* protein lacking 59 amino acids from the N terminus, though containing the Dof domain, is capable of binding DNA in vitro and activating transcription in a transient assay (Kang and Singh, 2000). However, *OBP3*'s subcellular localization is unknown. To determine the subcellular localization of *OBP3*, the same *OBP3* cDNA used by Kang and Singh (2000) was translationally fused to green fluorescent protein (GFP). This construct was cogenerated into onion (*Allium cepa*) epidermal cells along with a construct containing dsRed under control of the *Zea mays*

ubiquitin (UBQ) promoter. This dsRed control localized throughout the cell, including within the nucleus (Figure 2A), in a manner similar to constitutively expressed GFP (data not shown). However, the *OBP3*-GFP fusion protein was only nuclear localized in these onion epidermal cells (Figures 2B and 2C). *OBP3*'s nuclear localization (Figures 2A to 2C), along with its ability to bind DNA and activate transcription (Kang and Singh, 2000), suggests that this gene encodes a bona fide Dof transcription factor.

Tissue-Specific Localization of OBP3 Is Regulated by Light

OBP3 mRNA levels were not altered in seedlings grown in continuous light or in the dark (Figure 1E). In addition, *OBP3* transcript levels were unaffected by the fluence rate or wavelength of light or during the transition (first 24 h) from darkness to growth in the light (data not shown). However, many transcription factors involved in light signaling are regulated at the protein level (Osterlund et al., 2000; Bauer et al., 2004).

To determine the relative amount and localization of *OBP3* in response to changes in light, wild-type *Arabidopsis* was transformed with a construct encoding an *OBP3*: β -glucuronidase

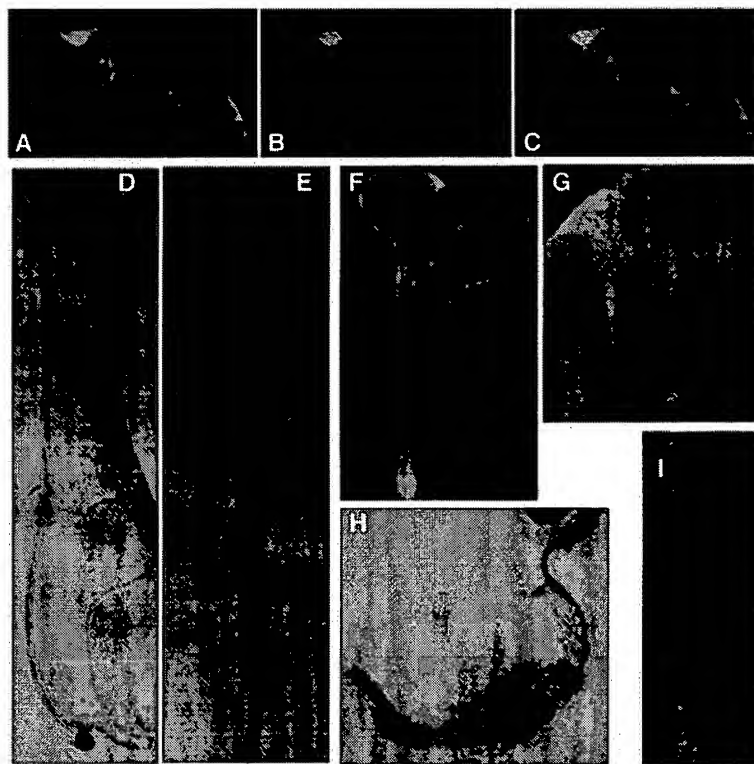


Figure 2. Subcellular and Tissue-Specific Localization of *OBP3*.

(A) to (C) Onion epidermal cells were cogenerated with constructs containing either UBQ:dsRed (A) or 35S:OBP3-GFP (B). The two images are merged to show the subcellular localization of *OBP3* (C).

(D) to (I) Wild-type *Arabidopsis* was transformed with a T-DNA containing genomic DNA encoding *OBP3* translationally fused to the *GUS* gene. Expression of this fusion gene was controlled by \sim 1.4 kb of DNA 5' of the *OBP3* gene. *OBP3*:*OBP3*-GUS localization was observed in 5-d-old seedlings grown either in the dark (D) and (E) or in continuous white light (F) to (I). GUS staining was observed in the apex and cotyledons of dark-grown seedlings (D) and (E). In light-grown seedlings, GUS staining was observed in the apex (F) and (I) and in the vascular tissue of the cotyledons (G) and (H), hypocotyl (F) and (I), and roots (H).

(GUS) translational fusion protein, consisting of the genomic DNA encoding *OBP3* fused at the 3' end to *GUS*. This fusion was expressed using 1.4 kb of DNA 5' of the *OBP3* open reading frame. Multiple homozygous lines containing a single locus insertion had varying degrees of *sob1-D* mutant phenotypes. These phenotypes correlated with *OBP3-GUS* mRNA levels, suggesting that the fusion protein is functional (see Supplemental Figure 1 online).

GUS analysis was performed on at least three independent lines grown for 5 d in the dark or in continuous white light (Figures 2D to 2I). GUS staining was present in the apex, cotyledons, and occasionally in the root apex of dark-grown seedlings (Figures 2D and 2E). In light-grown seedlings, GUS staining was present in the shoot apex (Figures 2F and 2I) and the vascular tissue of the cotyledons (Figures 2F and 2G), hypocotyl (Figures 2F and 2I), and roots (Figure 2H). Taken together, these data indicate that light causes *OBP3* to accumulate in the vascular tissue of hypocotyls and roots and possibly cotyledons. This localization was independent of the fluence rate of light (data not shown). Seedlings grown in continuous red or blue light showed similar staining patterns to white light-grown seedlings (data not shown). Seedlings grown in far-red light had staining only in the apex and cotyledons, similar to dark-grown seedlings (data not shown).

OBP3-RNAi Hypocotyls Are Less Responsive to Red Light in a *phyB*-Dependent Manner

The *sob1-D phyB-4* mutant suppressed the long-hypocotyl phenotype of *phyB-4* in the light, while elongating normally in the dark, suggesting that *OBP3* may be involved in light signaling (Figure 1). Because no null mutations in *OBP3* exist to date, *OBP3* partial-loss-of-function transgenic lines were generated using RNA interference (RNAi) (Hutvagner and Zamore, 2002) to further test the role of *OBP3* in photomorphogenesis. A 475-bp region containing a portion of the final *OBP3* exon and 3' untranslated region was amplified by PCR and cloned into a binary vector in a hairpin manner, under the control of the 35S promoter of *Cauliflower mosaic virus*. This region did not contain the highly conserved Dof domain, and BLAST analysis indicated no homology to other sequences in the *Arabidopsis* genome.

Some of the resulting homozygous *OBP3-RNAi* lines conferred larger adult stature (Figure 3). RT-PCR was performed on these plants to determine if they had lower *OBP3* transcript levels. Those lines with larger adult stature had lower *OBP3* expression (Figure 3). In addition, transgenic lines with normal adult stature had normal *OBP3* expression levels (data not shown). One of these original lines, *OBP3-RNAi1-4-3*, was crossed with the *sob1-D phyB-4* mutant, resulting in F1 progeny with a hypocotyl phenotype similar to the wild type (data not shown). This provides further evidence that *OBP3* expression is reduced in the *OBP3-RNAi* lines because the RNAi phenotype is dominant with regard to the overexpression phenotype.

To determine whether *OBP3* is involved in light signal transduction, fluence rate response experiments were performed using the wild type and the *OBP3-RNAi1-4-3* line (Figure 4). Like the *sob1-D* mutant, *OBP3-RNAi1-4-3* and other *OBP3-RNAi* lines elongated normally in the dark (Figures 1A and 4; see Supplemental Figure 2A online). In multiple fluence rates of white

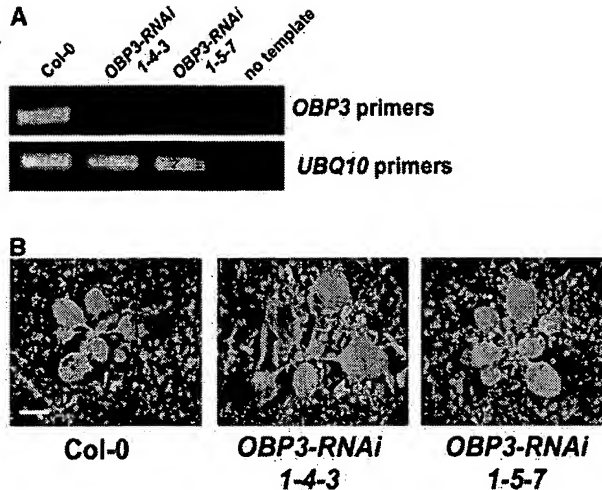


Figure 3. Identification of the *OBP3-RNAi* Mutants.

(A) Total RNA was isolated from 5-d-old seedlings grown in continuous white light. PCR was performed on cDNA by amplifying with *OBP3*-specific primers for 32 cycles. cDNA was normalized by amplifying with *UBQ10* primers for 24 cycles.

(B) The wild type and *OBP3-RNAi* homozygous, single locus insertion lines were grown in long-day growth conditions for 3 weeks. Bar = 10 mm.

light, *OBP3-RNAi1-4-3* conferred a subtle though statistically significant long-hypocotyl phenotype when compared with the wild type, suggesting that *OBP3* is involved in light signaling (Figure 4A). Multiple *OBP3-RNAi* lines, including *OBP3-RNAi1-4-3*, were also less responsive to multiple fluence rates of red light when compared with the wild type (Figure 4B; see Supplemental Figure 2A online). Multiple *OBP3-RNAi* lines, including *OBP3-RNAi1-4-3*, responded normally to far-red light (Figure 4D; see Supplemental Figure 2A online). Though hypocotyls of the *OBP3-RNAi1-4-3* line were shorter in blue light (Figure 4C), this phenotype was not conferred by other *OBP3-RNAi* lines (see Supplemental Figure 2A online). Together, these data indicate that *OBP3* is a positive regulator of hypocotyl elongation inhibition in red and white light.

To determine if *phyB* is necessary for this *OBP3*-mediated hypocotyl response in red light, double mutants between *OBP3-RNAi1-4-3* and weak and null alleles of *phyB* were generated. Although *phyB-null* mutants grown in red light are near their maximal growth rate, *phyA phyB* double mutants and *phyB phyC phyD* triple mutants are capable of elongating more than *phyB-null* mutants (Reed et al., 1994; Casal and Mazzella, 1998; Neff and Chory, 1998; Monte et al., 2003), suggesting that this genetic test will determine if *phyB* is required for the *OBP3*-mediated hypocotyl response. The *OBP3-RNAi1-4-3* hypocotyls were less responsive to red light only when wild-type or partially functional (i.e., *phyB-4*) *phyB* was present (Figure 5). By contrast, the *OBP3-RNAi1-4-3 phyB-null* (*phyB-9*) double mutant hypocotyls responded the same way to red light as the *phyB-9* mutant. This experiment was repeated in a lower fluence rate of red light and gave the same result (19 μ M/m²/s; data not shown),

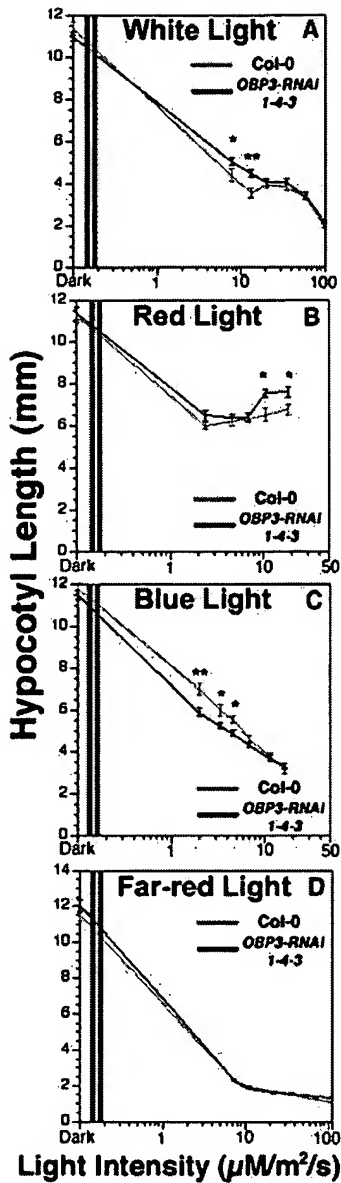


Figure 4. Fluence Rate Response Analysis for Hypocotyl Length of the *OBP3-RNAi1-4-3* Mutant.

Five-day-old seedlings were grown in the dark or varying fluence rates of continuous white (A), red (B), blue (C), and far-red (D) light. Bars = ± 1 SE. (*) equals $P < 0.5$, and (**) equals $P < 0.001$ from a Student's unpaired two-tail *t* test comparing the *OBP3-RNAi* mutant and the wild type from the same light treatment.

demonstrating that the *OBP3-RNAi1-4-3* aberrant hypocotyl response to red light requires phyB. Because *PHYB* transcript accumulation was not affected by the genetic state of *OBP3* (data not shown), these results demonstrate that this transcription factor is a positive regulator of phyB-mediated hypocotyl elongation inhibition in response to red light.

OBP3 Is a Negative Regulator of *cry1*-Mediated Cotyledon Expansion in Response to Blue Light

The *sob1-D phyB-4* double mutant had smaller, upwardly cupped cotyledons when grown in white light (Figures 1A and 6A). Because the *sob1-D* mutant was a severe dwarf as an adult (Figure 1B), it was predicted that *OBP3-RNAi* adult plants would be larger in stature. In addition to this larger adult stature (Figure 3), multiple *OBP3-RNAi* mutants had larger cotyledons when grown in white light (Figure 6; see Supplemental Figure 2B online). To determine if this increase in cotyledon size is because of cell expansion or cell division, epidermal imprints were examined and cell area was measured (Figure 6B, Table 1). The *sob1-D phyB-4* mutant cotyledons had smaller epidermal cells when compared with both the *phyB-4* mutant and the wild type (Figures 6A and 6B). *OBP3-RNAi1-4-3* and other *OBP3-RNAi* lines had larger epidermal cells when compared with the wild type (Figure 6B, Table 1).

To determine if *OBP3*-mediated cotyledon expansion involves specific photoreceptor signaling pathways, multiple *OBP3-RNAi* lines, including *OBP3-RNAi1-4-3*, were grown in different wavelengths of light, and the cotyledon area was measured (Figure 7; see Supplemental Figure 2B online). Cotyledons of the *OBP3-RNAi* lines were dramatically larger than the wild type in blue light and slightly, though significantly, larger in red and far-red light (Figure 7; see Supplemental Figure 2B online). Taken together, these data demonstrate that *OBP3* is a negative regulator of cotyledon expansion in multiple photomorphogenic signaling pathways.

The most striking *OBP3-RNAi* cotyledon phenotype was seen in blue light, suggesting a role for *cry1* in this response. To

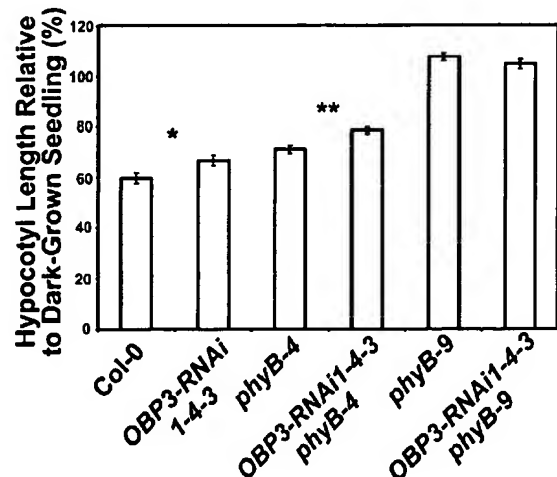


Figure 5. Photoreceptor Double Mutant Analysis for Hypocotyl Length.

Five-day-old seedlings were grown in the dark or continuous red light (29 $\mu\text{M}/\text{m}^2/\text{s}$). The *phyB-9* allele is a *phyB*-null mutant, and the *phyB-4* allele is a *phyB*-missense mutant. The hypocotyls of the dark-grown double mutant were longer when compared with the wild type, so the data are normalized to the average dark-grown hypocotyl length for each line. Bars = ± 1 SE. (*) equals $P < 0.5$, and (**) equals $P < 0.001$ from a Student's unpaired two-tail *t* test comparing the mutant with its control.

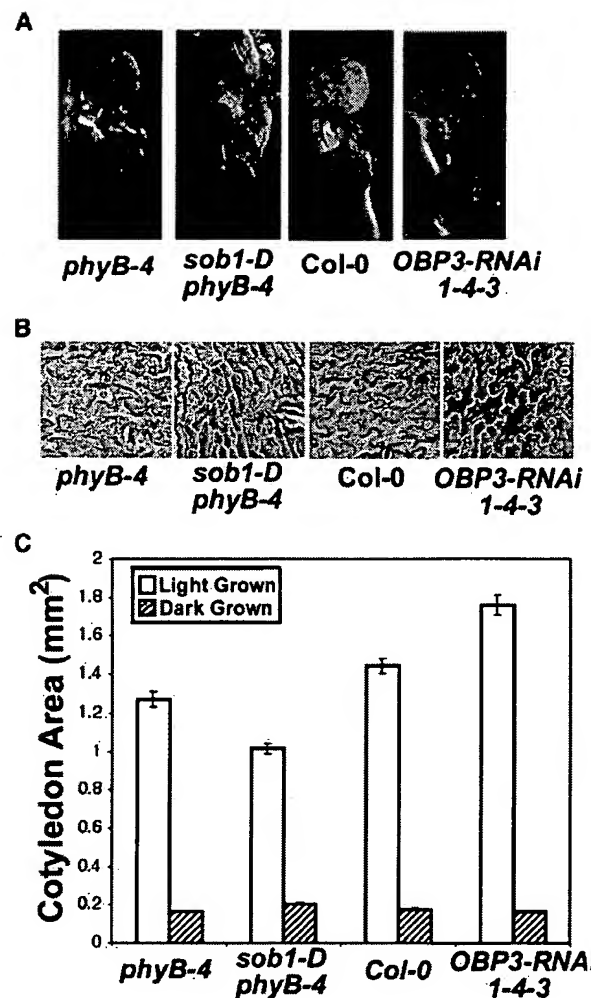


Figure 6. Cotyledon Cell Expansion in White Light.

(A) Photographs of cotyledons from seedlings grown in continuous white light for 5 d.

(B) Epidermal imprints of cotyledons from seedlings grown in continuous white light for 5 d.

(C) Cotyledon area from 5-d-old seedlings grown in the dark or continuous white light (35 $\mu\text{M}/\text{m}^2/\text{s}$). Error bars = $\pm 1 \text{ SE}$.

determine if *cry1* is necessary for the aberrant cotyledon response conferred by *OBP3-RNAi1-4-3* in blue light, double mutants were generated with weak and null alleles of *cry1*. The *OBP3-RNAi1-4-3 cry1-weak* (*cry1-102*) double mutant had significantly larger cotyledons than *cry1-102*. By contrast, cotyledons of the *OBP3-RNAi1-4-3 cry1-null* (*cry1-103*) double mutant were the same size as the *cry1-103* mutant. Thus, *OBP3*-mediated cotyledon expansion in response to blue light was observed only when wild-type or partially functional *cry1* (i.e., *cry1-102*) was present (Figure 7A). Because *CRY1* transcript accumulation was not affected by the genetic state of *OBP3* (data not shown), these data indicate that *OBP3* is a negative regulator of *cry1*-mediated cotyledon cell expansion in response to blue light.

DISCUSSION

Previous studies of transgenic plants overexpressing the Dof transcription factor, *OBP3*, have suggested that it is involved in plant growth and development (Kang and Singh, 2000). Here, we have identified *OBP3* in an activation-tagging mutant screen as an overexpression suppressor of the long-hypocotyl phenotype of a *phyB* missense allele (Figure 1). Seedlings of this *sob1-D* mutant elongate normally in the dark, with aberrant phenotypes conferred only in light-grown plants, suggesting that *OBP3* is involved in photomorphogenesis.

Earlier studies have shown that *OBP3* binds specifically to the Dof recognition sequence, A/TAAAG, in vitro and can activate transcription in a transient assay (Kang and Singh, 2000). We have now shown that *OBP3* is nuclear localized (Figures 2A to 2C), providing further evidence that this protein is a bona fide transcription factor. Though gene overexpression studies suggest a role for *OBP3* in plant development, the true function of this gene is unclear. To determine *OBP3*'s role in planta, we have used an RNAi approach to identify multiple *OBP3* partial-loss-of-function transgenic lines. Genetic and phenotypic analysis of these *OBP3-RNAi* lines has identified a complex role for *OBP3* in seedling photomorphogenesis.

There is precedence for other Dof transcription factors being involved in light signaling. *COG1* expression levels are induced in response to far-red and red light, and this regulation requires *phyA* and *phyB*, respectively (Park et al., 2003). In addition, transgenic lines with reduced *COG1* levels are more responsive to both red and far-red light, suggesting that this gene is a negative regulator of multiple phytochrome signaling pathways. *DAG1* and *DAG2* have opposing affects during seed germination in response to red light, acting as a repressor and activator, respectively (Papi et al., 2000, 2002; Gualberti et al., 2002). Dof involvement in light signaling is not limited to *Arabidopsis* because transcript levels and the ability to bind DNA of maize *DOF1* are also regulated by light (Yanagisawa and Sheen, 1998). Herein, we have shown that *OBP3* represents another Dof transcription factor involved in multiple aspects of light signaling, modulating both phytochrome- and cryptochrome-mediated seedling photomorphogenesis.

New Role for the Dof Transcription Factor OBP3 in Light Signaling

Fluence rate response experiments using *OBP3-RNAi* lines uncover *OBP3*'s involvement in light-mediated inhibition of hypocotyl elongation. Though the *OBP3-RNAi* lines responded normally to blue and far-red light, they were less responsive to

Table 1. Cotyledon Epidermal Cell Area

Genotype	Cotyledon Epidermal Cell Area μm^2 (SE)
Col-0	3.91 (0.11)
<i>OBP3-RNAi1-4-3</i>	5.02 (0.16)
<i>OBP3-RNAi1-5-7</i>	4.79 (0.19)

Seedlings were grown in continuous white light (35 $\mu\text{M}/\text{m}^2/\text{s}$) for 5 d.

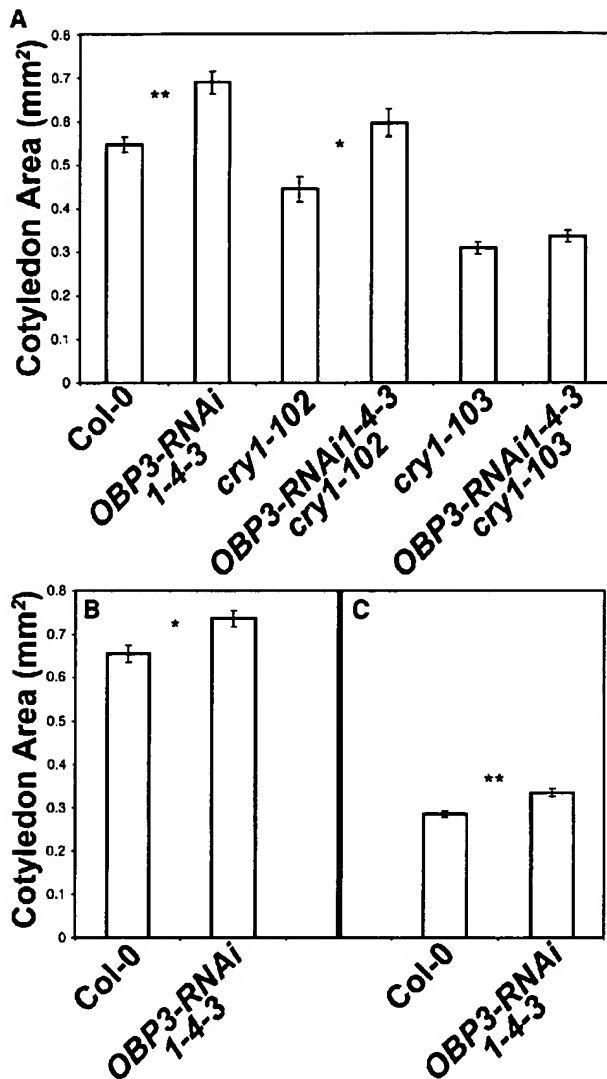


Figure 7. Cotyledon Expansion in Response to Different Wavelengths of Light.

(A) Cotyledon area from 5-d-old seedlings grown in continuous blue light (17 $\mu\text{M}/\text{m}^2/\text{s}$). The *cry1-102* allele is a *cry1-missense* mutant, and the *cry1-103* allele is a *cry1-null* mutant.

(B) Cotyledon area from 5-d-old seedlings grown in continuous red light (29 $\mu\text{M}/\text{m}^2/\text{s}$).

(C) Cotyledon area from 5-d-old seedlings grown in continuous far-red light (33 $\mu\text{M}/\text{m}^2/\text{s}$). Error bars = ± 1 SE. (*) equals $P < 0.5$, and (**) equals $P < 0.001$ from a Student's unpaired two-tail *t* test comparing the mutant with its control.

multiple fluence rates of white and red light (Figure 4; see Supplemental Figure 2A online). Double mutant analysis with one of these *OBP3-RNAi* lines, *OBP3-RNAi 1-4-3*, demonstrates that the aberrant hypocotyl phenotype in red light requires a functional phyB. Taken together, these data place OBP3 in

a red light signaling pathway, acting as a positive regulator of phyB-mediated inhibition of hypocotyl elongation.

In addition to causing subtle, though statistically significant, aberrant hypocotyl phenotypes, the genetic state of *OBP3* has a strong effect on light-dependent cotyledon expansion (Figure 6, Table 1; see Supplemental Figure 2B online), with the most dramatic response seen in blue light (Figure 7; see Supplemental Figure 2B online). The aberrant cotyledon phenotype of the *OBP3-RNAi 1-4-3* transgenic line in blue light requires a functional cry1 (Figure 7A), demonstrating that OBP3 is a negative regulator of cry1-dependent cotyledon expansion in blue light.

Like OBP3, the photoreceptors, including phyA, phyB, and cry1, affect cotyledon expansion in blue light (Neff and Chory, 1998). Aside from these photoreceptors, Ser/Thr Protein Phosphatase 7 (PP7) is the only other identified signaling component involved in blue light-mediated cotyledon expansion (Moller et al., 2003). Mutations in the photoreceptors and in transgenic lines with reduced PP7 levels have smaller cotyledons in blue light, suggesting they are each positive regulators of cotyledon expansion (Neff and Chory, 1998; Moller et al., 2003). To date, OBP3 is the only signaling component identified that negatively regulates cotyledon expansion in blue light (Figure 7A).

In addition to this cry1-mediated cotyledon expansion phenotype, OBP3 acts as a positive regulator of phyB-mediated

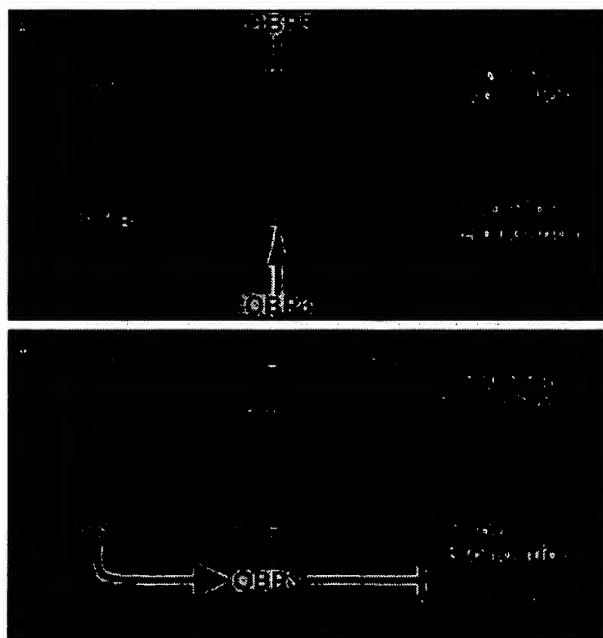


Figure 8. Possible Models Describing OBP3's Involvement in phyB and cry1 Signaling.

(A) OBP3 acts as a negative regulator of cry1-mediated cotyledon expansion in blue light and a positive regulator of phyB-mediated inhibition of hypocotyl elongation in red light.

(B) OBP3 is a negative regulator of expansion in the cotyledons and elongation in the hypocotyl. This regulation is modulated both negatively and positively by cry1 and phyB, respectively.

inhibition of hypocotyl elongation in red light. Other components have been identified that are involved in both phytochrome and cryptochrome signaling. Loss-of-function mutations in the basic helix-loop-helix transcription factor, *HFR1* (also called *RSF1* and *REP1*) cause reduced deetiolation responses in the hypocotyl when grown in far-red and blue light (Fairchild et al., 2000; Fankhauser and Chory, 2000; Soh et al., 2000; Duek and Fankhauser, 2003). A null mutation in the Ca^{2+} binding protein, *SUB1*, causes hypersensitivity of the hypocotyl to blue light and far-red light (Guo et al., 2001). Unlike *HFR1* and *SUB1*, which are involved in the *phyA* and *cry1* pathways, *OBP3* represents a connection between *phyB* and *cry1* signal transduction.

Current models of photomorphogenesis suggest that both early and late signal transduction pathways exist (Quail, 2002; Bauer et al., 2004). We propose that *OBP3* is involved in late photomorphogenic signaling events for several reasons. First, the genetic state of *OBP3* did not affect photoreceptor mRNA accumulation (data not shown), suggesting that *OBP3* operates downstream of these photoreceptors. In addition, *OBP3* transcript levels are unaffected by light (Figure 1E), and the changes in tissue-specific localization of an *OBP3:OBP3-GUS* translational fusion do not occur during the first 24 h after transition from darkness to growth in white light (data not shown). Finally, *OBP3*'s involvement in multiple photomorphogenic pathways (Figures 5 and 7) suggests that it acts downstream of photoreceptor signal integration.

Based on the data presented here, we propose a model where *OBP3* operates as a positive regulator of *phyB*-mediated hypocotyl elongation inhibition in red light and a negative regulator of *cry1*-mediated cotyledon expansion in blue light (Figure 8A). Other photomorphogenic signaling components can also have opposite roles in different responses. For example, *PIF3*, a basic helix-loop-helix transcription factor, acts as both a positive and negative regulator of phytochrome signaling. *PIF3* is a negative regulator of hypocotyl elongation inhibition, cotyledon opening, and expansion and a positive regulator of *CHS* transcript accumulation (Kim et al., 2003; Bauer et al., 2004).

An alternative model is that *OBP3* acts as a general negative regulator of cell/tissue expansion, with the photoreceptors differently regulating this response (Figure 8B), because *OBP3-RNAi* lines are larger as both seedlings and adults (Figures 3, 4, and 6). These two models are not mutually exclusive, as an existing model of hypocotyl elongation proposes two forces controlling growth: one promoting and one opposing (Parks et al., 2001). A similar mechanism may be regulating cotyledon expansion, and the photoreceptors, acting in part through *OBP3*, may be modulating these forces to control growth during photomorphogenesis (Figure 8).

One mode of action through which *OBP3* may function is via hormone signaling pathways. There are several hormones (e.g., auxin, brassinosteroids, and gibberellins) involved in cell expansion that are interconnected with light signaling during photomorphogenesis (Halliday and Fankhauser, 2003; Neff et al., 2005). Multiple suppressors of the long-hypocotyl phenotype of *phyB* mutants have been identified, which are involved both photomorphogenesis and hormone signaling (Reed et al., 1998; Neff et al., 1999). *BAS1/CYP72B1* (for *phyB-4* activation-tagged suppressor 1/cytochrome P450 72B1) inactivates active brassino-

steroids, acting as a modulator of photomorphogenesis through hormone inactivation (Neff et al., 1999; Turk et al., 2003). Gain-of-function mutants in the Auxin/Indole Acetic Acid Induced (Aux/IAA) gene, *Suppressor of Long Hypocotyl 2 (SHY2)/IAA3*, have deetiolation phenotypes in the dark and hyperresponsive hypocotyls in white light (Reed et al., 1998). In addition, this mutation in *SHY2/IAA3* affects auxin-dependent root growth, lateral root formation, and the gravitropic response, suggesting that *SHY2/IAA3* modulates both light and auxin signaling pathways (Tian and Reed, 1999). Interestingly, *OBP3* transcript levels are dramatically induced in response to auxin and salicylic acid (Kang and Singh, 2000), suggesting that this gene may also be acting as a point of interaction between light and hormone signaling. Future experiments will explore *OBP3*'s possible involvement in hormone signaling as a means of modulating photomorphogenesis.

METHODS

Growth Conditions and Light Sources

Seeds were surface sterilized by shaking in 70% (v/v) ethanol containing 0.05% (v/v) Triton X-100 for 15 min, followed by treatment with 95% (v/v) ethanol for 5 min. After the ethanol washes, seeds were dried on sterile 70-mm Whatman filter paper (Maidstone, UK) in a laminar-flow hood and sown on media containing either 0.8% phytagar (w/v) (Gibco BRL, Gaithersburg, MD), half-strength MS salts (Invitrogen, Carlsbad, CA), 1.5% (w/v) sucrose with antibiotic, or 1.0% phytagel (Sigma-Aldrich, St. Louis, MO), half-strength MS salts. After incubation for 4 d at 4°C, germination was induced by treating seeds with 1 h of red light followed by 23 h of darkness. Seeds were then placed in the appropriate light condition. All incubators were at 25°C.

Plates were incubated in a white light chamber (Model E-30-B; Percival Scientific, Perry, IA) or a light emitting diode incubator (Model E-30-LED; Percival Scientific). White light was supplied by four fluorescent tubes (F17T8/TL741 17 W; Phillips, Eindhoven, The Netherlands) and two incandescent bulbs (PC, 13,487 25T10/F CD 25 W, 120 V; GE, Fairfield, CT). Red and blue lights were supplied by eight fluorescent tubes. Colored Plexiglas was placed on the plates to obtain blue and red light conditions. Far-red light was obtained by the far-red light emitting diodes from the E-30-LED incubator. These diodes were set at 10% of their maximal fluence rate. One to five layers of fiberglass window screen were placed over the plates to obtain the appropriate fluence rates of light.

Activation-Tagging Mutagenesis

Arabidopsis thaliana phyB-4 mutant plants, ecotype Columbia (Col-0) were transformed with the activation-tagging construct, pSKI074 (GenBank accession number AF218466) (Weigel et al., 2000) as in Neff et al. (1999). Plants were transformed via the floral dip method using *Agrobacterium tumefaciens* strain GV3101 (Clough and Bent, 1998). T1 seeds were grown on plates containing kanamycin (30 mg/L) in continuous white light (35 $\mu\text{M}/\text{m}^2/\text{s}$) for 7 d. The *sob1-D phyB-4* double mutant was identified by its shorter hypocotyl when compared with *phyB-4* mutant plants. T2 seeds from self-fertilized *sob1-D phyB-4* were screened on plates with and without kanamycin to confirm that the mutant phenotype is linked to the transgene. T2 seedlings segregated 3:1 kanamycin resistant:kanamycin sensitive, indicating that there was one locus containing a T-DNA. T3 seeds from self-fertilized T2 plants were screened in the same way to confirm the genetic heritability of the mutant phenotype.

and linkage to the transgene. The presence of the *phyB-4* mutation was confirmed in the *sob1-D phyB-4* mutant as in Neff et al. (1999).

Cloning of the OBP3 Gene

DNA gel blot analysis and plasmid rescue were performed essentially the same as in Neff et al. (1999). The DNA gel blot indicated that the *sob1-D phyB-4* mutant contains only one T-DNA insertion. The location of this T-DNA was determined by cloning the flanking genomic DNA via plasmid rescue. Genomic DNA from the *sob1-D* mutant was digested with *Hind*III and religated with T4 DNA ligase (New England Biolabs, Beverly, MA), resulting in a 14.4-kb construct, pSOB1-H4. The genomic DNA flanking the T-DNA was sequenced with a primer (5'-GCTCTCTGAGGTC-GACGG-3'). BLASTn analysis indicated that the genomic DNA is from chromosome III, and the closest open reading frame was *OBP3* (At3g55370).

RT-PCR Analysis

RT-PCR analysis was performed on total RNA isolated, using the RNeasy Plant Mini kit (Qiagen, Valencia, CA), from 5-d-old seedlings grown in continuous white light. Total cDNA was synthesized using SuperScript III first-strand synthesis system for RT-PCR (Invitrogen). PCR was performed on dilute cDNA using Taq polymerase (Invitrogen). The *OBP3* gene was amplified using the 5'-TACTTCTGCCCAAGTTACTCAAACCC-TAGC-3' and 5'-GAATGAGAGATGGCCTGTTGAGTTGGAGG-3' primers. The *ubiquitin10* (*UBQ10*) gene was used as an internal control. *UBQ10* was amplified using the 5'-GGTATTCCCTCCGGACCAGCAGC-3' and 5'-CGACTTGTCAATTAGAAAGAGATAACAGGAACGG-3' primers. The linear range of accuracy for the detection of each transcript was established by comparing samples run for different numbers of cycles. All final RT-PCR experiments were performed at least in duplicate.

Recapitulation of the *sob1-D* Mutant Phenotype

The *sob1-D* recapitulation construct was generated by ligating a *Sac*I fragment from pSOB1-H4 into pPZP212 (Hajdukiewicz et al., 1994) cut with *Sac*I. This *Sac*I fragment from pSOB1-H4 contains the four enhancer elements from the CaMV 35S promoter, the *OBP3* open reading frame, and 4.1 kb of noncoding DNA 5' of the *OBP3* gene. The *phyB-4* mutant was transformed with this construct via *A. tumefaciens*-mediated transformation (Clough and Bent, 1998). Primary transformants were screened on plates containing kanamycin (30 mg/L).

Construction of the 35S:OBP3-GFP Fusion and Particle Bombardment

The *OBP3* cDNA lacking 59 N-terminal amino acids was amplified from cDNA synthesized from the *sob1-D* mutant using the following primers: 5'-CATGCCATGGATGGTGGAACGTGAACGTGCTCGG-3' and 5'-ACATGCCATGGCGAATGAGAGATGGCCTG-3'. The PCR product was cut with *Nco*I and inserted into the pCAMBIA1301 vector (CAMBIA, Canberra, Australia). This C-terminal fusion to GFP results in an Ala added onto the C terminus of *OBP3* in place of the stop codon. The PCR product was sequenced to confirm that there were no errors affecting the open reading frame.

Particle bombardment has been described in detail elsewhere (Zentella et al., 2002). The 35S:OBP3-GFP construct was cobombarded with a construct containing the dsRed gene driven by the maize (*Zea mays*) ubiquitin promoter (Zentella et al., 2002). These two constructs in a 1:1 molar ratio were cobombarded into layers of white onion (*Allium cepa*) cut into 1-inch squares. After bombardment, the onions were wrapped in moist Kim-Wipes and incubated in the dark for 24 h.

To view the transformed epidermal cells, the epidermal layer was pulled from the piece of onion with forceps and placed on a microscope slide. The layer of epidermal cells was kept moist with distilled water. The cells were viewed by confocal microscopy using the Leica confocal system TCS2 (Leica Microsystems, Heidelberg, Germany) essentially the same as by Zentella et al. (2002). At least 10 independent transformation events were observed, and all showed the same localization patterns.

Construction of the OBP3:OBP3-GUS Fusion Construct and GUS Analysis

The entire *OBP3* gene along with a small portion of the region upstream of the gene was amplified from pSOB1-H4 using the following primers: 5'-TTGCTCCGACCAATGTTTC-3' and 5'-ACATGCCATGGCGAATGAGATGGCCTG-3'. The fragment was cut with *Eco*RI and *Nco*I and inserted into pCAMBIA1381 (CAMBIA), cut with these same enzymes. This C-terminal fusion to GUS resulted in an Ala linking the two proteins. This portion of the construct, which was created by PCR, was sequenced to ensure that there were no errors. A 1438-bp region upstream of the *OBP3* gene is used to drive the expression of this fusion gene. This region was cloned from the pSOB1-H4 vector by cutting with *Eco*RI and inserted into the vector containing the *OBP3* open reading frame:GUS translational fusion gene, resulting in pJW8. *Arabidopsis* ecotype Col-0 was transformed with pJW8, and multiple homozygous, single locus insertion lines were identified by screening on plates containing hygromycin (20 mg/L).

GUS analysis was performed in triplicate on 5-d-old seedlings by incubating in GUS staining solution (1 mM 5-bromo-4-chloro-3-indolyl-β-D-glucuronic acid, cyclohexyl ammonium salt, 50 mM NaHPO₄, pH 7.2, and 0.05% [v/v] Triton X-100) at 37°C for 24 h. Seedlings were photographed essentially the same as by Turk et al. (2003). Lines 8.47.1, 8.7.2, and 8.83.1 were used in the analysis, and all showed similar GUS staining patterns (see Supplemental Figure 1 online).

Construction of OBP3-RNAi Construct

Primers 5'-CGCGGATCCGTGAAGCGGAAGAGAATG-3', 5'-CCATC-GATCATACATATCACCCACACCTC-3' and 5'-GACCTCGAGTGAAG-CGGAAGAGAATG-3', 5'-CGGGGTACCATACATATCACCCACACCTC-3' were used to amplify a 475-bp fragment of the *OBP3* gene and 3' untranslated region. These fragments were cloned into the pHANNIBAL vector (CSIRO Plant Industry, Victoria, Australia) in the sense direction with *Ava*I and *Kpn*I and in the antisense direction using *Cla*I and *Bam*HI. The resulting vector was cut with *Nos*I and cloned into the *Nos*I site of the pART27 binary vector (CSIRO Plant Industry). The resulting binary vector, pJW4, was transformed into the *A. tumefaciens* strain GV3101. *Arabidopsis* ecotype Col-0 was transformed with pJW4, and multiple homozygous, single locus insertion lines were identified by screening on plates containing kanamycin (30 mg/L).

Genetic Analysis

All mutant lines used in this study are *Arabidopsis* ecotype Col-0. The *cry1-102* and *cry1-103* alleles are described by Liscum and Hangarter (1991), Mockler et al. (1999), and Neff et al. (2002). The *phyB-9* allele is described by Reed et al. (1998). Double mutants were obtained by crossing and growing seeds on kanamycin-containing plates. F2 seeds were grown in the appropriate light conditions to identify homozygous photoreceptor mutants. Putative double mutants were confirmed in the F3 generation by growing on kanamycin-containing plates to identify lines homozygous for the *OBP3-RNAi* T-DNA. The photoreceptor mutations were confirmed by PCR analysis using the following primer pairs for each mutation: *cry1-102*, 5'-TCTCATCCGGCATCGACCAAC-3' and 5'-GGG-GAAGAAAGCGTGAATTTTCTGAATT-3'; *cry1-103*, 5'-AAGCTTC-TTGTAAAGCTTCAATTACCATGGAG-3', 5'-CGTATTACCAATT-

GGATCAAACTTGTACCCCTTC-3', and 5'-TTGGTCTCCTGGATGGAGT-AATGGTATAAAG-3'; *phyB-9*, 5'-CAATGTAGCTAGTGGAAAGAAGCTC-GATGTGG-3' and 5'-ACATAACAGTGTCTGCGTTCTCAAAACGC-3'.

The *cry1-102* PCR product was cut with *Eco*RI to distinguish between the wild-type and mutant alleles. The primers used to genotype the *cry1-103* mutation amplify two products for the wild-type allele and one product for the mutant allele. The *phyB-9* PCR product was cut with *Msp*I to distinguish between wild-type and mutant alleles.

Fluence Response and Cotyledon Area Measurements

To measure hypocotyl length, 5-d-old seedlings were removed from plates and laid on acetate sheets. The seedlings were digitized with a flatbed scanner at a resolution of 600 dpi. Cotyledons were placed on transparent tape and digitized as above. The hypocotyls and cotyledons were measured using ImageJ 1.29J (National Institutes of Health, Bethesda, MD; <http://rsb.info.nih.gov/ij/java/1.3.1>). All experiments were done in triplicate ($n \geq 30$) on media with and without sucrose. The data reported is from experiments on media without sucrose.

Epidermal Imprints and Epidermal Cell Area Measurements

Five-day-old seedlings grown in continuous white light were used for epidermal imprints. Imprints were taken by coating the top of the cotyledon with clear fingernail polish. After drying, the polish was removed with transparent tape. The tape was fastened to a microscope slide, and the imprint was viewed and photographed at 200 \times using the Nikon Eclipse E600 microscope (Tokyo, Japan), QImaging Retiga Ex camera (Burnaby, BC, Canada), and OpenLab 3.1.4 software (Lexington, MA). At least six cotyledons from each of three replicate experiments were digitized. The area from between five and 10 epidermal cells from each cotyledon was measured using ImageJ 1.29J (National Institutes of Health).

ACKNOWLEDGMENTS

We thank Quetzal Torres, Sarah Galanti, and Emily Gamelin for their technical assistance; Rodolfo Zentella for supplying dsRed construct and technical advice concerning particle bombardment; Barbara Kunkel, Eric Richards, Robert Kranz, Christian Fankhauser, Leeann Thornton, Ian Street, Edward Turk, and JingYu Zhang for their critical review of this manuscript. This work was directly supported by the Department of Energy (Grant DE-FG02-02ER15340 to M.M.N.). We are also grateful for support from the National Science Foundation (Grant 0114726 to M.M.N.) and the Monsanto Corporation (Grant 46011J to M.M.N.). M.A.D. was supported in part by the National Science Foundation Research Experience for Undergraduates (Grant 0114726 to M.M.N.).

Received September 15, 2004; accepted November 11, 2004.

REFERENCES

Ahmad, M., and Cashmore, A.R. (1993). HY4 gene of *A. thaliana* encodes a protein with characteristics of a blue-light photoreceptor. *Nature* **366**, 162–166.

Altschul, S.F., Gish, W., Miller, W., Myers, E.W., and Lipman, D.J. (1990). Basic local alignment search tool. *J. Mol. Biol.* **215**, 403–410.

Bauer, D., Viczian, A., Kircher, S., Nobis, T., Nitschke, R., Kunkel, T., Panigrahi, K.C., Adam, E., Fejes, E., Schafer, E., and Nagy, F. (2004). Constitutive photomorphogenesis 1 and multiple photoreceptors control degradation of phytochrome interacting factor 3, a transcription factor required for light signaling in *Arabidopsis*. *Plant Cell* **16**, 1433–1445.

Briggs, W.R., and Christie, J.M. (2002). Phototropins 1 and 2: Versatile plant blue-light receptors. *Trends Plant Sci.* **7**, 204–210.

Casal, J.J., and Mazzella, M.A. (1998). Conditional synergism between cryptochrome 1 and phytochrome B is shown by the analysis of *phyA*, *phyB* and *hy4* simple, double, and triple mutants in *Arabidopsis*. *Plant Physiol.* **118**, 19–25.

Clough, S.J., and Bent, A.F. (1998). Floral dip: A simplified method for *Agrobacterium*-mediated transformation of *Arabidopsis thaliana*. *Plant J.* **16**, 735–743.

Duek, P.D., and Fankhauser, C. (2003). HFR1, a putative bHLH transcription factor, mediates both phytochrome A and cryptochrome signalling. *Plant J.* **34**, 827–836.

Elich, T.D., and Chory, J. (1997). Biochemical characterization of *Arabidopsis* wild-type and mutant phytochrome B holoproteins. *Plant Cell* **9**, 2271–2280.

Fairchild, C.D., Schumaker, M.A., and Quail, P.H. (2000). HFR1 encodes an atypical bHLH protein that acts in phytochrome A signal transduction. *Genes Dev.* **14**, 2377–2391.

Fankhauser, C., and Chory, J. (2000). RSF1, an *Arabidopsis* locus implicated in phytochrome A signaling. *Plant Physiol.* **124**, 39–45.

Fankhauser, C., Yeh, K.C., Lagarias, J.C., Zhang, H., Elich, T.D., and Chory, J. (1999). PKS1, a substrate phosphorylated by phytochrome that modulates light signaling in *Arabidopsis*. *Science* **284**, 1539–1541.

Franklin, K.A., Praekelt, U., Stoddart, W.M., Billingham, O.E., Halliday, K.J., and Whitlam, G.C. (2003). Phytochromes B, D, and E act redundantly to control multiple physiological responses in *Arabidopsis*. *Plant Physiol.* **131**, 1340–1346.

Gualberti, G., Papi, M., Bellucci, L., Ricci, I., Bouchez, D., Camilleri, C., Costantino, P., and Vittorioso, P. (2002). Mutations in the Dof zinc finger genes DAG2 and DAG1 influence with opposite effects the germination of *Arabidopsis* seeds. *Plant Cell* **14**, 1253–1263.

Guo, H., Mockler, T., Duong, H., and Lin, C. (2001). SUB1, an *Arabidopsis* Ca^{2+} -binding protein involved in cryptochrome and phytochrome coaction. *Science* **291**, 487–490.

Hajdukiewicz, P., Svab, Z., and Maliga, P. (1994). The small, versatile pPZP family of *Agrobacterium* binary vectors for plant transformation. *Plant Mol. Biol.* **25**, 989–994.

Halliday, K.J., and Fankhauser, C. (2003). Phytochrome-hormonal signalling networks. *New Phytol.* **157**, 449–463.

Hutvagner, G., and Zamore, P.D. (2002). RNAi: Nature abhors a double-strand. *Curr. Opin. Genet. Dev.* **12**, 225–232.

Jarillo, J.A., Capel, J., Tang, R.H., Yang, H.Q., Alonso, J.M., Ecker, J.R., and Cashmore, A.R. (2001). An *Arabidopsis* circadian clock component interacts with both CRY1 and *phyB*. *Nature* **410**, 487–490.

Kang, H.G., and Singh, K.B. (2000). Characterization of salicylic acid-responsive, *arabidopsis* Dof domain proteins: Overexpression of OBP3 leads to growth defects. *Plant J.* **21**, 329–339.

Kim, J., Yi, H., Choi, G., Shin, B., and Song, P.S. (2003). Functional characterization of phytochrome interacting factor 3 in phytochrome-mediated light signal transduction. *Plant Cell* **15**, 2399–2407.

Koomneef, M., Rolff, E., and Spruit, C.J.P. (1980). Genetic control of light-inhibited hypocotyl elongation in *Arabidopsis thaliana* (L.) Heynh. *Z. Pflanzenphysiol.* **100**, 147–160.

Lin, C., and Shalitin, D. (2003). Cryptochrome structure and signal transduction. *Annu. Rev. Plant Biol.* **54**, 469–496.

Lin, C., Yang, H., Guo, H., Mockler, T., Chen, J., and Cashmore, A.R. (1998). Enhancement of blue-light sensitivity of *Arabidopsis* seedlings by a blue light receptor cryptochrome 2. *Proc. Natl. Acad. Sci. USA* **95**, 2686–2690.

Liscum, E., and Hangarter, R.P. (1991). *Arabidopsis* mutants lacking blue light-dependent inhibition of hypocotyl elongation. *Plant Cell* **3**, 685–694.

Mas, P., Devlin, P.F., Panda, S., and Kay, S.A. (2000). Functional interaction of phytochrome B and cryptochrome 2. *Nature* **408**, 207–211.

Matsushita, T., Mochizuki, N., and Nagatani, A. (2003). Dimers of the N-terminal domain of phytochrome B are functional in the nucleus. *Nature* **424**, 571–574.

Mockler, T.C., Guo, H., Yang, H., Duong, H., and Lin, C. (1999). Antagonistic actions of *Arabidopsis* cryptochromes and phytochrome B in the regulation of floral induction. *Development* **126**, 2073–2082.

Moller, S.G., Kim, Y.S., Kunkel, T., and Chua, N.H. (2003). PP7 is a positive regulator of blue light signaling in *Arabidopsis*. *Plant Cell* **15**, 1111–1119.

Monte, E., Alonso, J.M., Ecker, J.R., Zhang, Y., Li, X., Young, J., Austin-Phillips, S., and Quail, P.H. (2003). Isolation and characterization of phyC mutants in *Arabidopsis* reveals complex crosstalk between phytochrome signaling pathways. *Plant Cell* **15**, 1962–1980.

Nagy, F., and Schafer, E. (2002). Phytochromes control photomorphogenesis by differentially regulated, interacting signaling pathways in higher plants. *Annu. Rev. Plant Biol.* **53**, 329–355.

Neff, M.M., and Chory, J. (1998). Genetic interactions between phytochrome A, phytochrome B, and cryptochrome 1 during *Arabidopsis* development. *Plant Physiol.* **118**, 27–35.

Neff, M.M., Fankhauser, C., and Chory, J. (2000). Light: An indicator of time and place. *Genes Dev.* **14**, 257–271.

Neff, M.M., Nguyen, S.M., Malancharuvil, E.J., Fujioka, S., Noguchi, T., Seto, H., Tsubuki, M., Honda, T., Takatsuto, S., Yoshida, S., and Chory, J. (1999). BAS1: A gene regulating brassinosteroid levels and light responsiveness in *Arabidopsis*. *Proc. Natl. Acad. Sci. USA* **96**, 15316–15323.

Neff, M.M., Street, I.H., Turk, E.M., and Ward, J.M. (2005). Interaction of light and hormone signaling to mediate photomorphogenesis. In *Photomorphogenesis in Plants*, 3rd ed., E. Schäfer and F. Nagy, eds (Boston: Kluwer Academic Publishers), in press.

Neff, M.M., Turk, E., and Kalishman, M. (2002). Web-based primer design for single nucleotide polymorphism analysis. *Trends Genet.* **18**, 613–615.

Ni, M., Tepperman, J.M., and Quail, P.H. (1998). PIF3, a phytochrome-interacting factor necessary for normal photoinduced signal transduction, is a novel basic helix-loop-helix protein. *Cell* **95**, 657–667.

Osterlund, M.T., Hardtke, C.S., Wei, N., and Deng, X.W. (2000). Targeted destabilization of HY5 during light-regulated development of *Arabidopsis*. *Nature* **405**, 462–466.

Papi, M., Sabatini, S., Altamura, M.M., Hennig, L., Schafer, E., Costantino, P., and Vittorioso, P. (2002). Inactivation of the phloem-specific Dof zinc finger gene DAG1 affects response to light and integrity of the testa of *Arabidopsis* seeds. *Plant Physiol.* **128**, 411–417.

Papi, M., Sabatini, S., Bouchez, D., Camilleri, C., Costantino, P., and Vittorioso, P. (2000). Identification and disruption of an *Arabidopsis* zinc finger gene controlling seed germination. *Genes Dev.* **14**, 28–33.

Park, D.H., Lim, P.O., Kim, J.S., Cho, D.S., Hong, S.H., and Nam, H.G. (2003). The *Arabidopsis* COG1 gene encodes a Dof domain transcription factor and negatively regulates phytochrome signaling. *Plant J.* **34**, 161–171.

Parks, B.M., Folta, K.M., and Spalding, E.P. (2001). Photocontrol of stem growth. *Curr. Opin. Plant Biol.* **4**, 436–440.

Quail, P.H. (2002). Photosensory perception and signalling in plant cells: New paradigms? *Curr. Opin. Cell Biol.* **14**, 180–188.

Reed, J.W., Elumalai, R.P., and Chory, J. (1998). Suppressors of an *Arabidopsis thaliana* phyB mutation identify genes that control light signaling and hypocotyl elongation. *Genetics* **148**, 1295–1310.

Reed, J.W., Nagatani, A., Elich, T.D., Fagan, M., and Chory, J. (1994). Phytochrome A and phytochrome B have overlapping but distinct functions in *Arabidopsis* development. *Plant Physiol.* **104**, 1139–1149.

Reed, J.W., Nagpal, P., Poole, D.S., Furuya, M., and Chory, J. (1993). Mutations in the gene for the red/far-red light receptor phytochrome B alter cell elongation and physiological responses throughout *Arabidopsis* development. *Plant Cell* **5**, 147–157.

Soh, M.S., Kim, Y.M., Han, S.J., and Song, P.S. (2000). REP1, a basic helix-loop-helix protein, is required for a branch pathway of phytochrome A signaling in *Arabidopsis*. *Plant Cell* **12**, 2061–2074.

Tian, Q., and Reed, J.W. (1999). Control of auxin-regulated root development by the *Arabidopsis thaliana* SHY2/IAA3 gene. *Development* **126**, 711–721.

Turk, E.M., Fujioka, S., Seto, H., Shimada, Y., Takatsuto, S., Yoshida, S., Denzel, M.A., Torres, Q.I., and Neff, M.M. (2003). CYP72B1 inactivates brassinosteroid hormones: An intersection between photomorphogenesis and plant steroid signal transduction. *Plant Physiol.* **133**, 1643–1653.

Weigel, D., et al. (2000). Activation tagging in *Arabidopsis*. *Plant Physiol.* **122**, 1003–1013.

Yanagisawa, S., and Sheen, J. (1998). Involvement of maize Dof zinc finger proteins in tissue-specific and light-regulated gene expression. *Plant Cell* **10**, 75–89.

Zentella, R., Yamauchi, D., and Ho, T.H. (2002). Molecular dissection of the gibberellin/abscisic acid signaling pathways by transiently expressed RNA interference in barley aleurone cells. *Plant Cell* **14**, 2289–2301.